Graphene Nanoribbon Crossbar Nanomesh

K. M. M. Habib, A. Khitun, A. A. Balandin, and R. K. Lake
Department of Electrical Engineering
University of California Riverside
Riverside, CA 92506 U.S.A.
khabib@ee.ucr.edu; akhitun@engr.ucr.edu

***Abstract*—Graphene nanoribbon crossbars exhibit negative differential resistance. This nonlinear current-voltage response can be exploited in a nanomesh geometry for high-density logic or memory. A 2xN crossbar array can store 3^N states. Proof-of-principle of a high functional density architecture exploiting the non-linear dynamics of graphene nanoribbon crossbars in a nanomesh geometry is demonstrated.**

Keywords- graphene; crossbar; NDR; NEGF; FIREBALL; multi-valued memory

I. INTRODUCTION

Lack of a bandgap in two-dimensional (2D) graphene [1-3] reduces its utility for conventional electronic device applications. One way of introducing a bandgap is to stack two monolayers to form a bilayer with a bandgap that can be tuned by creating a potential difference between the two layers [4-7].

Recently, we have shown that independently contacting a top and bottom nanoribbon of two overlapping GNRs results in negative differential resistance (NDR) [8]. A crossbar geometry is most suitable for high density integration of NDR nodes. Simulations of the geometry, shown in Fig. 1, show a current–voltage response plotted in Fig. 2 [9]. This functionality can be exploited in a crossbar GNR (xGNR) network utilizing the nonlinear elements for memory and logic applications.

II. GNR CROSSBAR DEVICE

The model cross-bar GNR (xGNR) structure consists of a vertical and a horizontal semi-infinite, H-passivated, relaxed, armchair type GNR (AGNR) placed one on top of the other at right angles as shown in Fig. 1. The widths of the GNRs are chosen to be 14-C atomic layers ($3n + 2$) ~1.8 nm to minimize the bandgap resulting from the finite width. The calculated bandgap of the 14-AGNR is

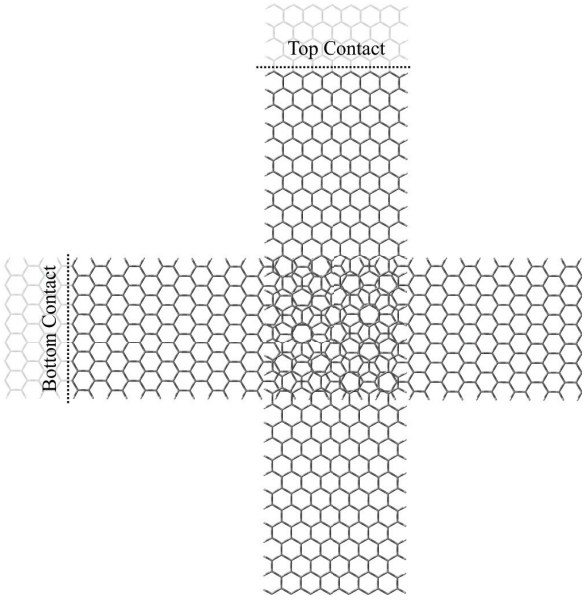

Figure 1: Atomistic geometry of the GNR crossbar. Two hydrogen passivated relaxed armchair GNRs are placed on top of each other at a right angles with a vertical separation of 3.35 Å . A bias is applied by independently contacting each GNR.

130 meV which is in good agreement with Son *et al*. [10].

The electronic structures of the GNRs and xGNR are modeled with the quantum molecular dynamics, DFT code, Fireball [11,12], using separable, nonlocal Troullier-Martins pseudopotentials [13], the BLYP exchange correlation functional [14, 15], a self-consistent generalization of the Harris-Foulkes energy functional [16 - 19] and a minimal sp^3 Fireball basis set. The radial cutoffs of the localized pseudoatomic orbitals forming the basis are r_c^{1s} = 4.10 Å for hydrogen and r_c^{2s} = 4.4 Å and r_c^{2p} = 4.8 Å for carbon [20]. Fireball Hamiltonian matrix elements are used in the NEGF algorithm to

978-1-4577-0995-1/11/$26.00 ©2011 IEEE

calculate the surface self-energies, Green's function of the device, the spectral function, the transmission, and the current as described in [20].

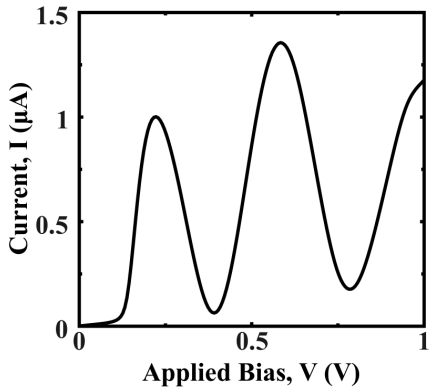

Figure 2: Simulated *I-V* characteristics of the crossbar structure exhibiting NDR. The first peak and the valley currents occur at 0.2 V and 0.4 V and the second peak and the valley currents occur at 0.6 V and 0.8 V respectively [9].

III. Cross-bar for Dynamic Memory & Logic

A graphene-based crossbar structure consisting of a number of vertical and horizontal GNRs opens a new horizon for building scalable and ultra-fast memory and logic devices. During the past decade, the crossbar has attracted much attention as a promising approach towards nanometer size architectures exploiting non-linear I-V characteristics at the point of cross junctions [21-25]. In the most cases, the cross-point is considered as a programmable diode. For example, a nanowire crossbar structure with a layer of rotaxane molecules serving as the programmable cross points has been experimentally demonstrated [26]. The NDR of the xGNR structure shown in Fig. 2 can be exploited in a network utilizing the collective dynamics of the nonlinear elements similar to the "neuromorphic" architecture described by V. P. Roychowdhury et al. [27].

A replica of the graphene 2-D crossbar structure comprising vertical GNRs (vGNRs) and horizontal GNRs (hGNRs) and the equivalent circuit are shown in Fig. 3(A) and (B), respectively. There is a 2-D net consisting of horizontal and vertical GNR layers. The vertical and horizontal

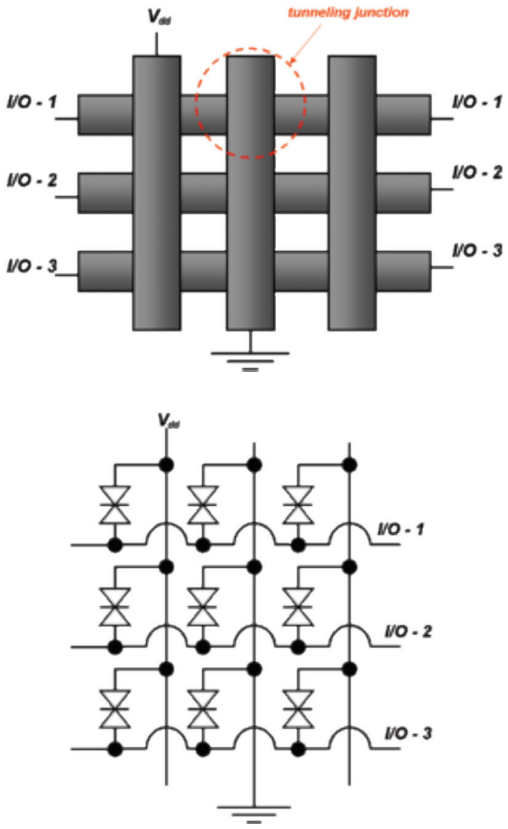

Fig.3 (Top) General view of the GNR cross-bar structure. consisting of vertical and horizontal GNRs. (Bottom) Equivalent circuit consisting of resonant tunneling diodes (RTDs).

layers are assumed to have a linear resistance, while the cross-points are modeled as identical resonant tunneling diodes. In order to illustrate the operation of the network, we carried out numerical simulations based on the piecewise approximation *I-V* characteristics (Fig.4). Assuming the slopes of the low and high voltage branches the same, the approximate tunneling *I-V* characteristic is described by the set of 4 parameters: V_p, I_p, V_v, I_v, which are the peak voltage, the peak current, the valley voltage and the valley current, respectively. Thus, for the GNR-junction, we assumed $V_p = 1$, $I_p = 1$, $V_v = 2$, $I_v = 0.01\ I_p$. In all graphs all voltages are normalized to $[V_p]$ and all currents are normalized to $[I^C_p]$, respectively. The capacitance of the crosspoint is assumed equal to the quantum capacitance value of 21 μF cm^{-2} [28].

The particular choice of tunneling parameters was made arbitrary to simulate the general features of the GNR-based network. The dynamics of the network is well described by the balance equations for the each point of junction as follows:

$$\frac{CdV_{i,j}}{dt} = -\left[J^{C}_{i,j} + J^{S}_{i,j} + \sum_{\substack{k,l \neq i,j \\ k,l \in R}} J^{D}_{ij,kl} \right] \qquad (1)$$

where $V_{i,j}$ is the potential, C is the capacitance, J^{C}, J^{S} and J^{D} are the vertical, horizontal and the tunneling currents, respectively. Each of these currents is defined by potential difference across the points on the mesh, where the subscripts i and j indicates the position in the 2-D lattice. The potentials of the vertical/horizontal edge contacts are considered as the boundary conditions. The model is suitable for logic performance illustration (e.g. output voltages as a function of the boundary conditions, read-in and read-out procedures, switching dynamics, etc.).

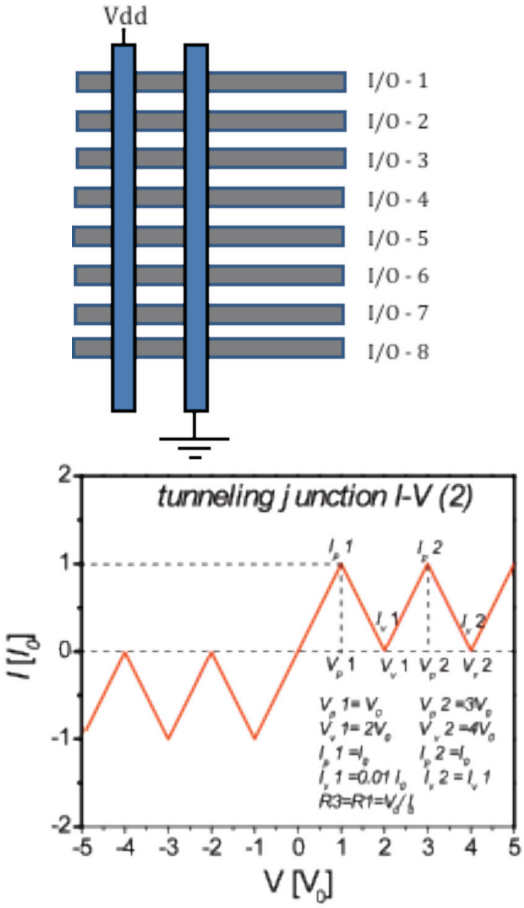

Fig.4 (Top) Schematic of the 2×8 GNR crossbar memory. (Bottom) Piecewise approximation to the xGNR *I-V* characteristic.

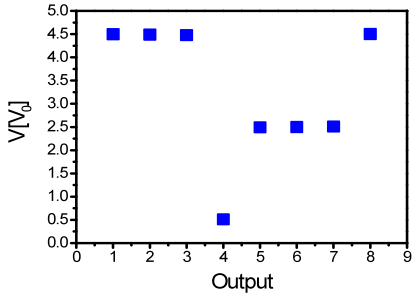

Fig. 5. Results of numerical simulations showing one out of 3^8 possible triple-state outputs (0.5V, 2.5V, and 4.5V @ Vdd=5V).

As an example of the network capabilities for multi-bit dynamic storage, we present the results of numerical modeling by Eq. 1. The voltages are applied to the vGNRs as shown in Fig. 4. In this case, each of the possible paths for the electric current consists of at least two cross-junctions. In turn, the potential of the each hGNR may have three stable states depending on the Vdd and the NDR characteristics. The results of numerical simulations in Fig. 5 illustrate one of the 3^8 possible output voltage combinations. The horizontal GNRs can be considered as the input/output ports for information read-in and read-out. The switching between the states on each node can be done independently from others by applying a voltage pulse to the hGNR. In this, case, a cross-bar comprising N hGNRs may store 3^N states.

The model xGNR structure has some promising performance matrices. The area of a single cross point is about 10nm x 10nmwith a geometrical capacitance of ~0.1 aF. The resistances at the first peak and valley currents are found to be ~200 kΩ and ~6 MΩ respectively. The typical RC time constant is then in the order of tens of femto

seconds making it suitable for high density terahertz applications. A series combination of two xGNRs, used in above analysis, has three stable points. Assuming V_{dd} = 1V, the average power dissipation at these stable points is ~0.5 μW. The slew rate, defined as the rate at which the output voltage can be changed from one stable point to other, is on the order of 10 THz.

The described graphene nanoribbon crossbar is of great potential for integration with conventional CMOS-based circuitry offering a novel logic unit with almost no area or time delay overhead. The use of the crossbar based on NDR devices has been discussed for a long-time [21-25]. Recent progress in graphene nanoribbon fabrication makes this approach feasible for practical applications. High mobility and nanometer scale size are the main advantages inherent to the graphene. This work presents the results of the theoretical study and numerical modeling aimed to illuminate the potential benefits of using a nanostructure comprising just two graphene nanoribbons.

IV. Conclusion.

In conclusion, proof-of-principle of a high functional density architecture exploiting the non-linear dynamics of graphene nanoribbon crossbars in a nanomesh geometry has been demonstrated. The possibility of building a multi-valued memory is illustrated by numerical modeling based on the simulated I-V characteristics of the crossbar structure exhibiting NDR. The GNR crossbar sketched here is an example of plausible architecture to benefit from the unique graphene properties. The described graphene nanoribbon crossbar can be evolved in different ways to make use of the collective dynamics inherent to networks consisting of NDR-base devices. Defect tolerance and integration with CMOS are among the main potential issues which require a more detailed study.

References

[1] K. S. Novoselov, A. K. Geim, S. V. Morozov, D. Jiang, M. I. Katsnelson, I. V. Grigorieva, S. V. Dubonos, and A. A. Firsov, "Two-dimensional gas of massless dirac fermions in graphene," Nature, vol. 438, no. 7065, pp. 197–200, November 2005.

[2] K. S. Novoselov, A. K. Geim, S. V. Morozov, D. Jiang, Y. Zhang, S. V. Dubonos, I. V. Grig-orieva, and A. A. Firsov, "Electric Field Effect in Atomically Thin Carbon Films," Science, vol. 306, no. 5696, pp. 666–669, 2004.

[3] T. Ando, "Exotic electronic and transport properties of graphene," Physica E: Low-dimensional Systems and Nanostructures, vol. 40, no. 2, pp. 213 – 227, 2007.

[4] K.-T. Lam and G. Liang, "An ab initio study on energy gap of bilayer graphene nanoribbons with armchair edges," Applied Physics Letters, vol. 92, no. 22, p. 223106, 2008.

[5] C. L. Lu, C. P. Chang, Y. C. Huang, J. M. Lu, C. C. Hwang, and M. F. Lin, "Low-energy electronic properties of the ab-stacked few-layer graphites," Journal of Physics: Condensed Matter, vol. 18, no. 26, p. 5849, 2006.

[6] H. Min, B. Sahu, S. K. Banerjee, and A. H. MacDonald, "Ab initio theory of gate induced gaps in graphene bilayers," Phys. Rev. B, vol. 75, no. 15, p. 155115, Apr 2007.

[7] Y. Zhang, T.-T. Tang, C. Girit, Z. Hao, M. C. Martin, A. Zettl, M. F. Crommie, Y. R. Shen, and F. Wang, "Direct observation of a widely tunable bandgap in bilayer graphene," Nature, vol. 459, no. 7248, p. 820, 2009.

[8] K. M. M. Habib, F. Zahid and R. K. Lake, "Negative differential resistace in bilayer graphene nanoribbons," Applied Physics Letters, vol. 98, no. 19, p. 192112, 2011.

[9] K. M. M. Habib and R. K. Lake, "Graphene nanoribbon crossbar resonant tunneling diode," (in preparation).

[10] Y.-W. Son, M. L. Cohen, and S. G. Louie, "Energy gaps in graphene nanoribbons," Phys. Rev. Lett., vol. 97, no. 21, p. 216803, 2006.

[11] O. F. Sankey and D. J. Niklewski, "Ab initio multicenter tight-binding model for molecular-dynamics simulations and other applications in covalent systems," Phys. Rev. B, vol. 40, no. 6, pp. 3979 – 3995, 1989.

[12] J. P. Lewis, K. R. Glaesemann, G. A. Voth, J. Fritsch, A. A. Demkov, J. Ortega, and O. F. Sankey, "Further developments in the local-orbital density-functional-theory tight-binding method," Phys. Rev. B, vol. 64, no. 19, p. 195103, 2001.

[13] J. L. Martins, N. Troullier, and S. H. Wei, "Pseudopotential plane-wave calculations for ZnS," Phys. Rev. B, vol. 43, no. 3, pp. 2213 – 2217, 1991.

[14] A. D. Becke, "Density-functional exchange-energy approximation with correct asymptotic behavior," Phys. Rev. A, vol. 38, no. 6, pp. 3098 – 3100, 1988.

[15] C. Lee, W. Yang, and R. G. Parr, "Development of the colle-salvetti correlation energy formula into a functional of the electron density," Phys. Rev. B, vol. 37, no. 2, pp. 785 – 789, 1988.

[16] J. Harris, "Simplified method for calculating the energy levels of weakly interacting fragments," Phys. Rev. B, vol. 31, pp. 1770–1779, 1985.

[17] W. M. C. Foulkes and R. Haydock, "Tight-binding models and density-functional theory," Phys. Rev. B, vol. 39, pp. 12 520–2536, 1989.

[18] A. A. Demkov, J. Ortega, O. F. Sankey, and M. P. Grumbach, "Electronic structure approach for complex silicas," Phys. Rev. B, vol. 52, no. 3, pp. 1618 – 1630, 1995.

[19] P. Jelinek, H. Wang, J. P. Lewis, O. F. Sankey, and J. Ortega, "Multicenter approach to the exchange-correlation interactions in ab initio tight-binding methods," Phys. Rev. B, vol. 71, no. 23, p. 235101, 2005.

[20] N. A. Bruque, M. K. Ashraf, T. R. Helander, G. J. O. Beran, and R. K. Lake, "Conductance of a conjugated molecule with carbon nanotube contacts," Phys. Rev. B, vol. 80, no. 15, p. 155455, 2009.

[21] S. C. Goldstein and M. Budiu, "NanoFabrics: Spatial Computing Using Molecular Electronics," Proc. Int'l Symp.Computer Architectures (ISCA 01), IEEE CS Press, 2001.

[22] Y. Luo et al., "Two-Dimensional Molecular Electronics Circuits," ChemPhysChem, vol. 3, no. 6, 2002, pp. 519-525. pp. 178-189.

[23] D. B. Strukov and K. K. Likharev, "CMOL FPGA: A Recon-figurable Architecture for Hybrid Digital Circuits with Two-Terminal Nanodevices," Nanotechnology, June 2005, pp. 888-900.

[24] A. DeHon, “Nanowire-Based Programmable Architectures,” ACM J. Emerging Technologies in Computing Systems, vol. 1, no. 2, 2005, pp. 109-162.

[25] G. S. Snider and R. S. Williams, “Nano/CMOS Archi- tectures Using a Field-Programmable Nanowire Interconnect,” Nanotechnology, Jan. 2007; http://iopscience.iop.org/0957-4484/18/3/035204.

[26] J. E. Green et al., “A 160-Kilobit Molecular Electronic Memory Patterned at 1011 Bits Per Square Centimetre,” Nature, 25 Jan. 2007, pp. 414-417.

[27] V. P. Roychowdhury et al., “Collective computational activity in self-assembled arrays of quantum dots: A novel neuromorphic architecture for nanoelectronics,” IEEE Trans. Electron Devices, vol. 43, no. 11, pp.1688–1699, Nov. 1996.

[28] Jilin Xia, Fang Chen, Jinghong Li and Nongjian Tao, “Measurement of the quantum capacitance of graphene”, Nat. Nanotech., 4, 505 (2009).